Strongly resonating bosons in hot nuclei

S. Zhang,[1,*] A. Bonasera,[2,3] M. Huang,[1,†] H. Zheng,[4] D. X. Wang,[1] J. C. Wang,[1] L. Lu,[1] G. Zhang,[5]
Z. Kohley,[2,6] Y. G. Ma,[5,7,8] and S. J. Yennello[2,6]

[1]*College of Physics and Electronics information, Inner Mongolia University for Nationalities, Tongliao, 028000, China*
[2]*Cyclotron Institute, Texas A&M University, College Station, Texas 77843, USA*
[3]*Laboratori Nazionali del Sud, INFN, via Santa Sofia, 62, 95123 Catania, Italy*
[4]*School of Physics and Information Technology, Shaanxi Normal University, Xian 710119, China*
[5]*Shanghai Advanced Research Institute, Chinese Academy of Sciences, Shanghai, 201210, China*
[6]*Chemistry Department, Texas A&M University, College Station, Texas 77843, USA*
[7]*Key Laboratory of Nuclear Physics and Ion-beam Application (MOE), Institute of Modern Physics,*
Fudan University, Shanghai, 200433, China
[8]*University of the Chinese Academy of Sciences, Beijing, 100080, China*

When two heavy ions near the Fermi energy collide, a warm and low-density region can form in which fragments appear. This region is mainly dominated by proton (p) and alpha (α) particles. In such an environment, the α particles interact with each other and, especially through strong resonances, form complex systems such as ^{8}Be and ^{12}C. Our experiments show that $^{70(64)}$Zn(^{64}Ni) + $^{70(64)}$Zn(^{64}Ni) reactions at $E/A = 35$ MeV/nucleon levels of ^{8}Be appear around relative energies $E_{ij} = 0.092$ MeV, 3.03 MeV as well as above 10 and 100 MeV. We propose a different method to derive the correlation function based on the relative transverse energy distribution to minimize the experimental uncertainties. For the 3α systems, multiresonance processes give rise to excited levels of ^{12}C. In particular, the Hoyle state at 7.654 MeV excitation energy shows a decay component through the ground state of ^{8}Be and also components where two different α couples are at relative energies consistent with the ground state of ^{8}Be at the same time.

I. INTRODUCTION

Several decades after the suggestion given by Fred Hoyle [1] of a 0^+ resonance near the 3α threshold to accelerate ^{12}C formation in stars, the Hoyle state (HS) is still a hot topic in nuclear structure [2–16]. While its energy, i.e., 7.654 MeV, and width, 8.5 eV, are firmly established, there are debates on its decay. It is commonly accepted [5–16] that almost 100% of the HS decay is through the ground state of ^{8}Be (^{8}Be$_{g.s.}$), thus corresponding to a sequential decay (SD), i.e., first an α particle is emitted, and then ^{8}Be decays into two α particles with 0.092 MeV relative kinetic energy. Other decay modes; for example, the theoretically predicted direct decay (DD) of ^{12}C into three α particles of equal energy (DDE) or into a linear chain (LD) [4,5] have been studied in high-precision, high-statistics experiments [8–16] giving an upper limit of 0.043% [14], 0.036% [15], and 0.024% [15] for DD, DDE, and LD, respectively. While we are probably at the limit of the experimental sensitivity, higher-statistics experiments might be performed, or different strategies might be explored. In this paper, we discuss a completely new approach, i.e., we generally explore the ^{12}C decays also in the presence of nearby nuclear matter. This is surely relevant since stellar processes, where ^{12}C (or larger nuclei) are formed, might

occur inside a dense star or on its surface, thus occurring under different conditions of density and temperature. One way to simulate some stellar conditions is to collide two heavy ions at beam energies near the Fermi energy. In central or peripheral collisions of the two ions, first we have a gentle increase in the density which is slightly above the ground-state density, $\rho_0 = 0.16$ fm^{-3} [17,18], as revealed by microscopic calculations and experiments [19–22]. The system expands while cooling, and for densities below $(1/3–1/6)\rho_0$, clusters start to appear; this is referred to as the freeze-out region. Not only are protons and alpha particles formed, but also nuclei of larger masses with neutron (N) and proton (Z) contents. Under such conditions, excited fragments might decay, and nearby small fragments might coalesce and form new nuclei. The study of the formation and decay of complex fragments in nuclear matter is of interest and, in particular, in this work, we will study the decay modes of ^{12}C and ^{8}Be in 3αs and 2αs, respectively. To increase the statistics, we combined the results of three different experiments: ^{70}Zn + ^{70}Zn, ^{64}Zn + ^{64}Zn, and ^{64}Ni + ^{64}Ni all at 35 MeV/nucleon [23] and checked that each system separately produced results in agreement with the others at least for the observables discussed in this paper. There are many reasons for studying decays in nuclear fragmentation, in particular the following:

(1) In nuclear matter, the levels and widths of decaying nuclei might be shifted or modified because of the

---

*zsylt@imun.edu.cn
†huangmeirong@imun.edu.cn

interaction with nearby species. For example, a change in the width of a resonance as compared with the vacuum might tell us the time duration of the freeze-out region.

(2) Levels not observed in a vacuum might appear in the surrounding medium, for example, if many α particles are formed at relative kinetic energies where $E_{ij} = 0.092$ MeV, which is the binding energy of the $^8\text{Be}_{\text{g.s.}}$, then strong resonances among these bosons could give rise to correlations and Bose–Einstein condensation (BEC) [22,24]. These conditions might be identified with the strong-resonance region in microscopic calculations of the structure of ^{12}C [5,20]. If this is a new state of ^{12}C as yet unobserved, it could be assigned as an Efimov state (ES). This is a general feature first predicted for nuclear systems [24,25] and only observed in atomic systems [26,27].

(3) Are the decay modes of a particular resonance modified in the medium? For example, is the SD of the HS still dominant with respect to the DD?

(4) The SD dominance of the HS tells us that the relative kinetic energy of two α particles is 0.092 MeV. What is the relative kinetic energy of the third α particle with respect to the first two? Why is the HS located at 7.654 MeV?

These and many other questions prompted us to follow an unconventional approach to nuclear structure and decay. The important tool is the detector, which must measure the energy and angle of fragments ejected from heavy-ion collisions to a high precision.

The paper is organized as follows: Section II summarizes the method of selecting and reconstructing events to analyze the important ingredients from relative-kinetic-energy distributions of 2αs. In Sec. III, we discuss further particular decay modes of ^{12}C. We conclude and summarize our work in Sec. IV.

II. METHOD AND RESULTS

We analyzed the data from the experiments performed at the Cyclotron Institute, Texas A&M University [21,23], using the NIMROD 4π detector [28]. Experimental details can be found in Refs. [20,21,23,28]. Here, it suffices to discuss the approach we follow in this paper. The detector measures the charge Z and mass A of each fragment up to $Z = 30$ and $A = 50$ on an event-by-event basis [23,29]. From all the collected events, we selected 3α events, and the analysis was performed only on them. The momenta of the α particles are rather well measured with the only major problem arising when the relative kinetic energy of the 2αs is small, on the order of tens of keV. Such particles are detected in two nearby detectors (or in the same one) of NIMROD, and because of the detector's finite granularity, an error results in the angle and consequently for the relative momenta. This is a problem for all detector types and the resulting error or minimum relative kinetic energy which can be measured is of the order of 40 keV [8,9]: the larger the granularity, the smaller the error. An evident advantage of our method, since we are working at

the beam energy close to the Fermi energy, is that each ion has high kinetic energy, larger than few MeV/nucleon [23,29]. This is optimal for our detector. It is the relative kinetic energy between α particles that needs to be small in order to reveal low energy excited levels of ^8Be and ^{12}C.

We emphasize that only the events with α multiplicity equal to three are analyzed in our analysis. Let us start by recalling the relation that calculates the excitation energy E^* of ^{12}C decaying into 3αs with Q value $Q = -7.275$ MeV. This relationship is given by

$$E^* = \frac{2}{3} \sum_{i=1, j>i}^{3} E_{ij} - Q, \qquad (1)$$

where E_{ij} is the relative kinetic energy of 2α and is measured event by event. Thus, we can easily estimate Eq. (1). Notice that the important ingredients entering Eq. (1) are the relative kinetic energies; since we have three indistinguishable bosons, we analyze the E_{ij} distribution by cataloging for each event the smallest relative kinetic energy, E_{ij}^{min}, the middle relative kinetic energy, E_{ij}^{Mid}, and the largest relative kinetic energy, E_{ij}^{Lar}.

In Fig. 1, we plot the relative-kinetic-energy distributions for these three cases. In the top panels, the solid black circles give the distributions obtained from the real events. They show bumps but no real structures. This is due to the fact that in the fragmentation region, some α may come from the decay of ^8Be or ^{12}C or they might come from completely noncorrelated processes; for example, the α emission from a heavy fragment [23,29]. To distinguish the correlated from the noncorrelated events, we randomly choose three different α from three different events and build the distributions displayed in Fig. 1 (mixing events—red open circles). The total number of real and mixing events are normalized to one, respectively. The two distributions look similar on a log-scale but show some remarkable differences at low relative kinetic energies. While the distribution of the real events in Fig. 1(a) goes down, it goes up in Figs. 1(b) and 1(c) when the relative energy is not large. As we have mentioned, when the relative kinetic energy becomes very small, it becomes difficult to assign the angle of detection because of the detector granularity. This is, of course, less important for the cases of Figs. 1(b) and 1(c) since the smallest relative kinetic energies are obtained for the events in the first panel. To correct this feature, we fit the highest points of Fig. 1(a) with an exponential function. This allows us to derive the instrumental error $\Delta E = 1/22$ MeV $= 0.045$ MeV; see Fig. 1(a). The estimated error is slightly larger than what is found in Refs. [8–16] but small enough to let us derive the results discussed below. For Figs. 1(b) and 1(c), it is evident that the experimental error is less important and a change in slope can be seen around 0.1 MeV (the $^8\text{Be}_{\text{g.s.}}$). To uncover the resonance, we can perform an exponential fit by using the same slope (or experimental error) as before and fit the experimental point at 0.045 MeV. By subtracting the fits from the real events, we obtain the open squares in Fig. 1, which can be considered as the real events corrected by the detector acceptance. As we can see, all three cases display a bump around 0.08 MeV (very close to 0.092 MeV),
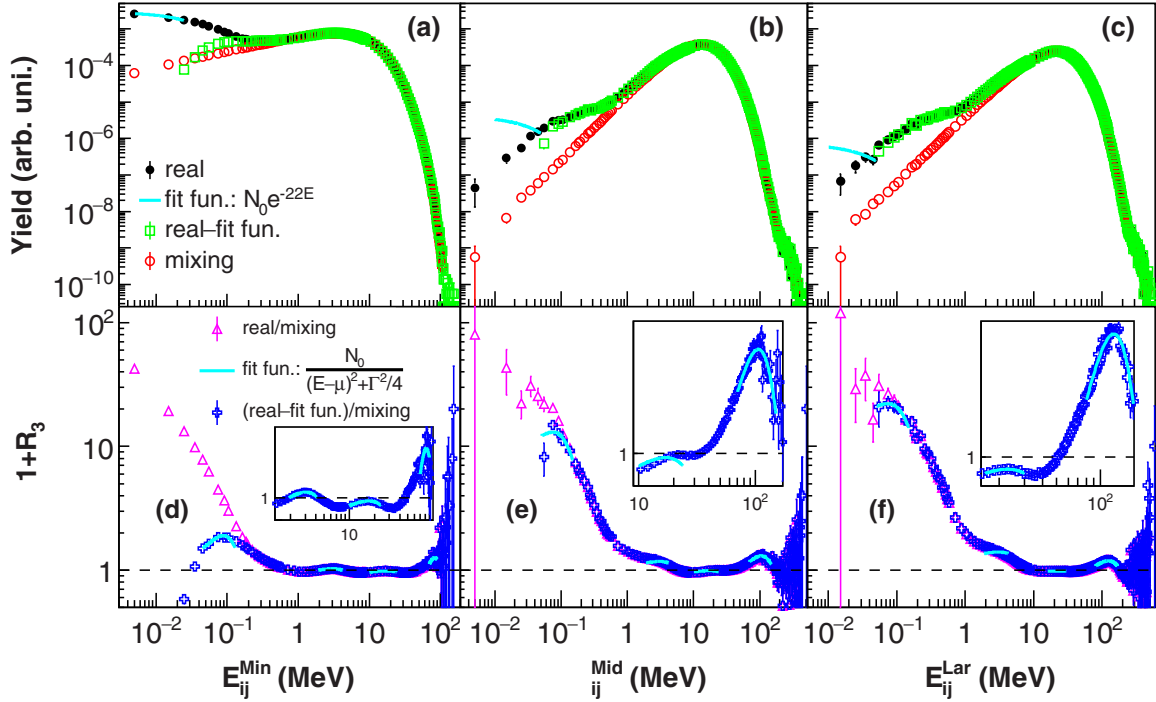
FIG. 1. Selected events from $^{70(64)}$Zn(^{64}Ni) + $^{70(64)}$Zn(^{64}Ni) at $E/A = 35$ MeV/nucleon with α multiplicity equal to three. Relative kinetic-energy distribution as a function of (a) the minimum relative kinetic energy, (b) the middle relative kinetic energy, and (c) the largest relative kinetic energy of 2αs. The solid black circles represent data from real events, the red open circles are from mixing events, and the green open squares represent the difference between the real events and the exponential function (solid line), which takes into account the experimental error. The ratios of the real (pink open triangles) data and the real data minus the fitting function (blue crosses) divided by the mixing events are, respectively, a function of (d) the minimum relative kinetic energy, (e) the middle relative kinetic energy, and (f) the largest relative kinetic energy of 2αs. The solid lines are Breit–Wigner fits.

corresponding to the decay of ^{8}Be$_{\text{g.s.}}$. Because of the way we have ordered relative kinetic energies of the the 2αs, we can deduce that, if the largest relative kinetic energy is 0.092 MeV, the other two must be 0.092 MeV as well (since they are smaller). Thus, we have events where the 3αs are in mutual resonance, which is a mechanism similar to the Efimov states where a boson is exchanged between the other two [24,25,30]. If this cannot be associated with a feature of a strongly resonating boson gas [5], it might be an unexplored state of ^{12}C at $E^* = 7.458$ MeV [as given by Eq. (1)]. In Ref. [31], the possibility of such a state was discussed, and it was suggested that its observation probability is eight orders of magnitude smaller than the HS. Of course those calculations were in a vacuum; when in a medium, the mechanism of mutual resonances might be enhanced in the presence of other fragments, which could be more complex bosons (for example, ^{16}O) or fermions (for example, ^{7}Li). Taking the ratio of the real (minus

the exponential fit) and the mixing events gives the correlation functions $1 + R_3$ displayed in the bottom panels of Fig. 1. The ratio shows that not only are peaks present around 0.08 MeV for all cases, but also at 3.05 MeV corresponding to the first excited level of ^{8}Be for the smallest relative kinetic energies, and higher-energy peaks are also visible.

A Breit–Wigner (BW) fit to these resonances gives the parameters reported in Table I. No clear peaks can be seen for the 3.05 and 17.0 MeV cases in Figs. 1(e) and 1(f). We used the same fitting values obtained in Fig. 1(d) for the 3.05 and 17.0 MeV cases in Fig. 1(e) and for the 3.05 MeV case in Fig. 1(f). For the largest relative-kinetic-energy case, Fig. 1(f), a peak appears around 23 MeV. As we can see, the centroids of the resonances are in good agreement with values in a vacuum, but the widths are somehow larger either due to the experimental acceptance or, most probably, to the presence of a medium. These differences from the vacuum

TABLE I. Parameters of BW fit to peaks in Fig. 1.

	E_{ij}^{Min}: μ (MeV)	$\hbar/\Gamma$ (fm/c)	E_{ij}^{Mid}: μ (MeV)	$\hbar/\Gamma$ (fm/c)	E_{ij}^{Lar}: μ (MeV)	$\hbar/\Gamma$ (fm/c)
Peak 1	0.088 ± 0.001	1192 ± 66	0.08 ± 0.02	1089 ± 288	0.08 ± 0.04	984 ± 540
Peak 2	3.05 ± 0.01	14.2 ± 0.3				
Peak 3	17.0 ± 0.1	2.08 ± 0.04			22.9 ± 0.3	1.1 ± 0.1
Peak 4	83 ± 3	2.8 ± 1.0	106 ± 1	0.95 ± 0.04	124.1 ± 0.9	0.70 ± 0.02

values are more marked for higher energies in the region of 10–20 MeV where we know there are many resonances in ^{8}Be. Some of these resonances have large widths and others have narrow widths [32]. Probably, when in a medium, the effects in the freeze-out region are responsible for this feature, and if the width is associated with the lifetime of the system, then we can derive the value $\tau = \hbar/\Gamma \cong 1$ fm/c. There are no reported levels of ^{8}Be (or ^{12}C) around 100 MeV; thus, we could associate these bumps with some or many unobserved new levels at high excitation energies. However, it should be noted that the corresponding excitation energy per particle of ^{12}C: $E^* = 100/12$ MeV $= 8.33$ MeV is very close to the center-of-mass energy in the heavy-ion collisions $E_{\text{c.m.}} = 35/4$ MeV $= 8.75$ MeV. Thus the correlation at such high energies might be due to the formation of a hot boson-fermion gas mixture and has been analyzed in some detail in Refs. [20–22]. A detector efficiency problem cannot be excluded since high-energy α particles move in the forward direction into the beam hole and thus remain undetected. The latter might be the correct explanation and is supported by the fact that the centroid energy changes for different relative energies; see the last row in Table I. The lifetime of such a system is of the order of 1 fm/c. It is interesting to notice that the quantity $1 + R_3$ is smaller than one in the energy region above 10 MeV and becomes larger than one around 100 MeV (recall that the real and mixing events are normalized to the same area).

III. DECAY MODES OF ^{12}C

In this work, the excitation energy E^* of ^{12}C from 3αs is also reconstructed by using Eq. (1). The excitation-energy distributions of the real events (solid black circles) and the mixing events (red open squares) are plotted in Fig. 2(a), and their ratio $(1 + R_3)$ (green open squares) in Figs. 2(b) and 2(c) with different energy windows. We can see that there is a sharp peak below $E^* = 8$ MeV. This feature is an effect of the finite granularity of the detectors that, especially at low relative excitation energies, are not able to reveal fine structures. We notice that, at high relative energies, the $1 + R_3$ is approximately equal to one, which indicates that the available phase space is dominated by statistical processes.
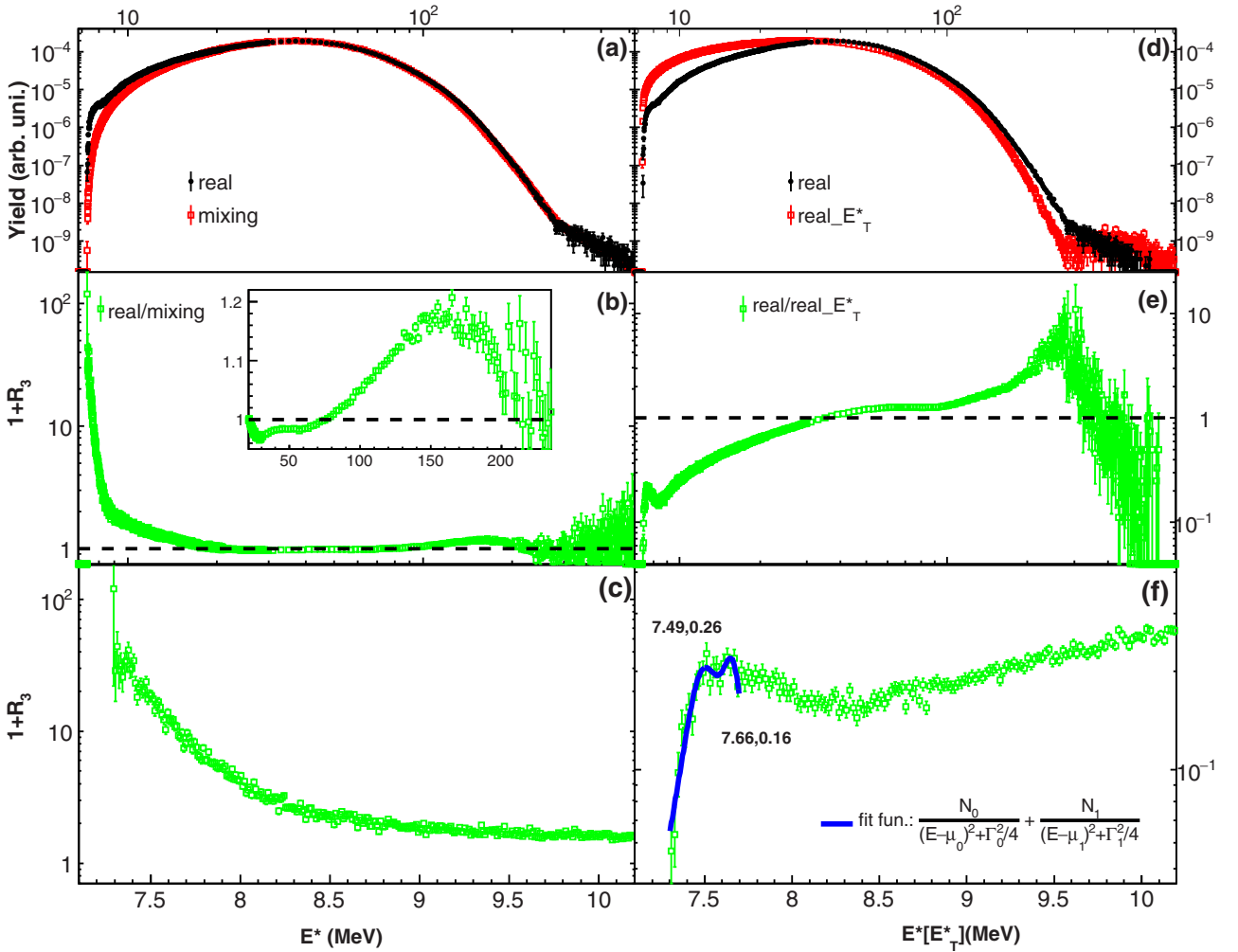

FIG. 2. The excitation-energy distributions of ^{12}C from 3αs. The solid black circles are the real events, red open squares are mixing events (or real transverse events), green open squares indicate the ratios of the real and mixing events (or real transverse events), and the blue solid line is the BW fit.

This feature suggested to us a different procedure to minimize the effects of the detector low granularity. In fact, if the system reaches thermal equilibrium, one can look at the α transverse relative-kinetic-energy distribution. The advantage of this procedure is that, instead of producing mixing events to derive the available phase space, we can derive the transverse kinetic-energy distribution from the same real events. When the ratio of the real events and the real transverse events is derived, the detector error might cancel out or becomes less important. This is a new method to study correlation functions. Similar to Eq. (1), we define the transverse excitation energy as

$$E_T^* = \frac{2}{3} \sum_{i=1, j>i}^{3} \frac{3}{2} \left(E_{ij}^X + E_{ij}^Y \right) - Q, \qquad (2)$$

where E_{ij}^X and E_{ij}^Y are the relative kinetic energy of 2α in the X and Y directions (Z is the beam axis direction).

In Figs. 2(d)–2(f), the transverse excitation energy of the real events (red open squares) is also included. We can see that there is a clear broad peak around 7.6 MeV in Fig. 2(f). From

the BW fit to this broad peak, the parameters of the centroids at 7.49 MeV (ES of ^{12}C) and at 7.66 MeV (HS of ^{12}C) are obtained.

To increase our confidence in the new proposed method, we reconstruct the excitation energy E^* of ^{3}Li from three proton events (see Fig. 3). We arbitrarily assign $Q = -7.275$ MeV, which is the Q value of ^{12}C for easy comparison to the 3α case. No peaks are observed when the transverse energy distribution is used, while the mixing technique shows a huge bump at low relative energies similar to the ^{12}C case leading to the conclusion that it is the detector finite acceptance which produces the "bump."

To strengthen the above results, we derived observables which give the probability of ^{12}C decay into a particular mode [say the 3α relative kinetic energies are equal (DDE) or two energies are equal and the third one is twice the sum of the first two (LD)] with respect to SD. These probabilities have been discussed experimentally using different techniques [8–16]; thus, it is especially interesting to compare our results in a medium with conventional approaches. Notice that the effects in a medium might be present in Ref. [9] and this
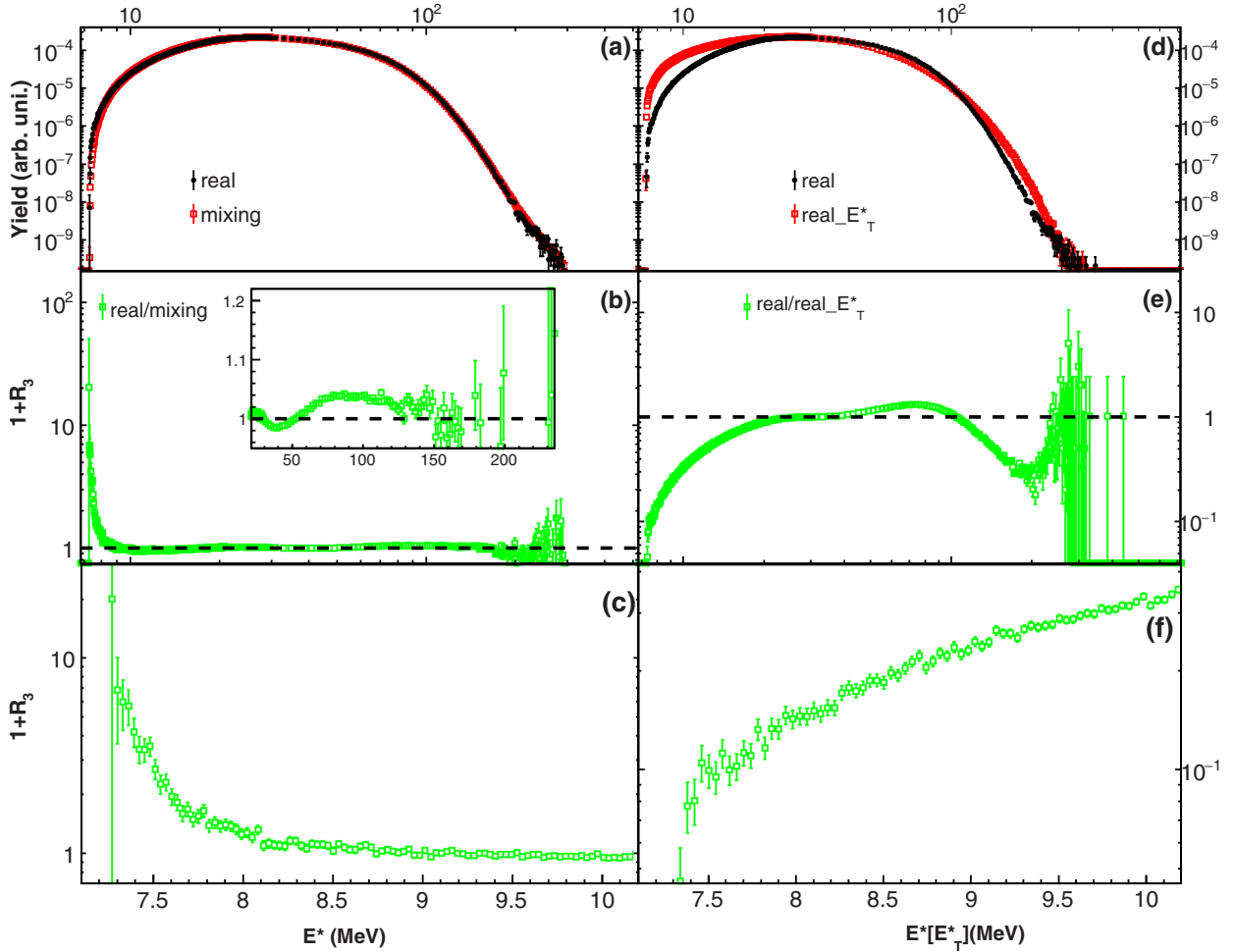

FIG. 3. The excitation-energy distributions of the ^{3}Li from three proton events, where we have arbitrarily assigned $Q = -7.275$ MeV for easy comparison to Fig. 2. The solid black circles are the real events, red open squares are mixing events (or real transverse events), green open squares indicate the ratios of the real and mixing events (left panels) or real transverse events (right panels).
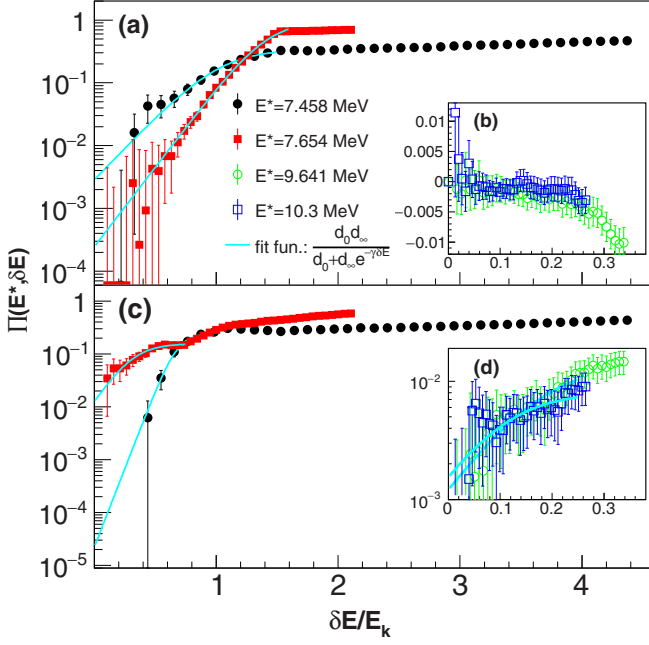
FIG. 4. The probability ratios of the DDE (top) and LD (bottom) as a function of the error [normalized to the kinetic contribution to E^* from Eq. (1)].

might explain the discrepancies from conventional approaches [8–16]. We define the decay probability as follows:

$$\prod(E^*, \delta E)$$
$$= \frac{\sum_{ij}[Y_R(\text{DDE or LD}, E_{ij}) - Y_M(\text{DDE or LD}, E_{ij})]}{\sum_{ij}[Y_R(\text{SD}, E_{ij}) - Y_M(\text{SD}, E_{ij})]},$$
$$(3)$$

where the sum is extended over all relative kinetic energies corresponding to a ^{12}C level with excitation energy E^* from Eq. (1) and variance δE, which we will vary to the smallest values allowed by the statistics. The $Y_R(\text{SD}, E_{ij})$ and $Y_M(\text{SD}, E_{ij})$ in the denominator are obtained by fixing the smallest relative kinetic energy to the ^{8}Be$_{\text{g.s.}} \pm \delta E/3$ for the real (R) and mixing (M) events, respectively. The yields of DDE or LD are obtained by opportunely choosing the relative kinetic energies in the numerator. For example, the DDE case is obtained by choosing three equal relative kinetic energies (within $\delta E/3$ for each one). For a fixed excitation energy, we can estimate Eq. (3) from the data by changing δE in order to derive the limiting value of the ratio compatible with the experimental sensitivity.

In Fig. 4, we plot the ratios for the DDE (top panel) and the LD (bottom panel) as a function of δE [normalized to the kinetic contribution to E^* from Eq. (1)]. The ES ($E^* = 7.458$ MeV) and the HS ($E^* = 7.654$ MeV) cases are given, respectively, by the solid (black) circles and the solid (red) squares. We have divided the ES cases by the HS SD, thus these ratios give the decay probabilities of the ES with respect to the HS. The 9.641 MeV (green open circles) and the 10.3 MeV (blue open squares) are given in the insets. The ratios can be reproduced by the function [33] given by

$$\prod(E^*, \delta E) = \frac{d_0 d_\infty}{d_0 + d_\infty e^{-\gamma \delta E}}.\qquad(4)$$

The parameter d_0 ($\delta E \rightarrow 0$) gives the smallest possible physical value of the ratios or the experimental error, while the largest value d_∞ ($\delta E \rightarrow \infty$) is connected to the available phase space [33]. The fit values of d_0 are reported in Table II and are compared with the data in the literature. Since Ref. [9] might contain effects from within a medium as in our case, we argue that the difference is due to not properly subtracting the mixing events when calculating the ratios, as in Eq. (3). Another possibility is the contribution of the ES due to the experimental sensitivity. We can see that the LD contribution of the ES is compatible with zero, which is consistent with the definition of the ES. For the larger excitation energies considered here, the ratios are negative for the DDE case [see Fig. 4(b)] and compatible with zero for the LD case [see Fig. 4(d)].

Not only the excited levels of ^{8}Be determine the SD modes of ^{12}C but also multiple integers of the ^{8}Be$_{\text{g.s.}}$ energy. In the left panels of Fig. 5, we plot the ratios for the HS when the ^{8}Be$_{\text{g.s.}}$ energy is consistent with $E_{ij}^{\min}$ and E_{ij}^{Mid} [Fig. 5(a)] or E_{ij}^{Mid} is twice ^{8}Be$_{\text{g.s.}}$ [Fig. 5(b)]. In the right panels of Fig. 5, the ratios are plotted for 9.641 and 10.3 MeV, when $E_{ij}^{\min} = 0.092$ MeV, $E_{ij}^{\text{Mid}} = E_{ij}^{\text{Lar}}$ [Fig. 5(c)], or $E_{ij}^{\text{Lar}} = 3.03$ MeV,

TABLE II. Fit values of the parameter d_0 compared with Refs. [5,9–13,15,31].

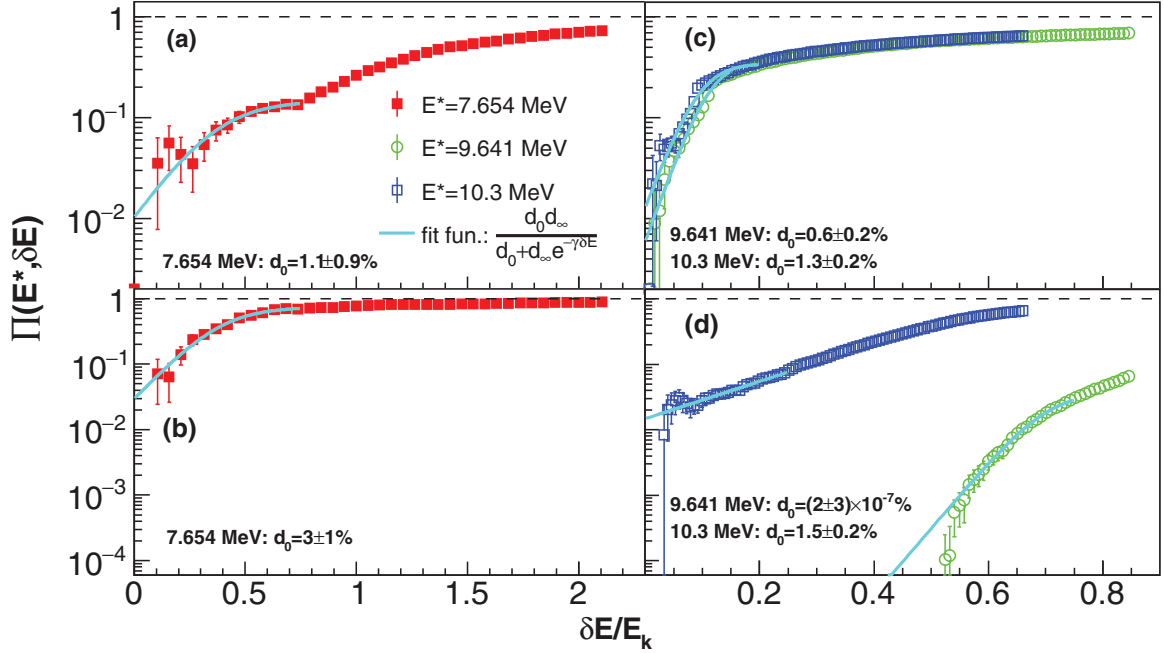|	ES : DDE (%)	ES : LD (%)	HS : DDE (%)	HS : LD (%)	9.641 : DDE (%)	9.641 : LD (%)	10.3 : DDE (%)	10.3 : LD (%)
Present	0.3 ± 0.1	0.002 ± 0.004	0.025 ± 0.005	1 ± 1	0	0.1 ± 0.1	0	0.2 ± 0.2
Ref. [9]			7.5 ± 4.0	9.5 ± 4.0	0			
Ref. [12]			0.3 ± 0.1	0.1				
Ref. [11]			0.45					
Ref. [15]			0.036	0.024				
Ref. [10]			0.09	0.09				
Ref. [13]			0.08					
Ref. [5]			0.005	0.03				
Ref. [31]			0.0036					

FIG. 5. The probability ratios of the HS (a) when the $^8Be_{g.s.}$ energy is consistent with two α relative kinetic energies, or (b) the second largest energy is twice of the $^8Be_{g.s.}$ energy. The ratios are plotted for 9.641 MeV (green open circles) and 10.3 MeV (blue open squares), (c) when $E_{ij}^{min} = 0.092$ MeV, $E_{ij}^{Mid} = E_{ij}^{Lar}$, or (d) $E_{ij}^{Lar} = 3.03$ MeV, $E_{ij}^{min} + E_{ij}^{Mid} = \frac{3}{2}(E^* + Q) - E_{ij}^{Lar}$.

$E_{ij}^{min} + E_{ij}^{Mid} = \frac{3}{2}(E^* + Q) - E_{ij}^{Lar}$ [Fig. 5(d)]. There are decay modes with those conditions; in particular, when the relative kinetic energies are approximately equal to the ratio $1 : 2 : 3$, a $3\% \pm 1\%$ contribution to the SD results for the HS; see Fig. 5(b).

IV. SUMMARY AND CONCLUSION

In this work, we discuss the energy levels of ^8Be and ^{12}C in hot nuclear matter. We found that the DDE and LD decay modes are strongly depleted. Thus the decay probability is mainly determined by the ^8Be formation probability in ^{12}C. Depending on the excitation energy of ^{12}C, ^8Be might be formed, not only in the ground state, but also in excited states as well. We confirm the finding of Ref. [34] that some decay modes are dominated by ^8Be levels hit more than once. A special case is the ES when the relative energies of 3αs are consistent with the $^8Be_{g.s.}$, a signature of a strongly resonating boson gas or an Efimov state, consistent with observations in atomic systems [27]. Some DDE and LD decay modes might be observed at very large excitation energies and these will be discussed further in a following presentation together with the question of BEC. We have discussed a method to obtain the correlation function by using the transverse relative kinetic energy instead of the mixing-events technique. This reduces the uncertainty due to the detector finite granularity, but ambiguities still remain, especially on the question of whether there might be a resonance in ^{12}C below the Hoyle state [31,35]. This "resonance" might be due to the 3αs going through the $^8Be_{g.s.}$ resonance at the same time, a mechanism introduced for Efimov states [24–27,35]. It might be an effect which occurs in hot nuclear matter only and not necessarily a new excited level in ^{12}C which could be tested in higher statistics experiments without in-medium effects. A dedicated experiment with higher statistics and better detector system, say for $^{40}Ca + ^{40}Ca$ collisions around 40 MeV/nucleon, should shed further light on the properties of the resonating bosons in hot matter.

[1] F. Hoyle, Astrophys. J., Suppl. Ser. **1**, 121 (1954).

[2] D. J. Marin-Lambarri, R. Bijker, M. Freer, M. Gai, T. Kokalova, D. J. Parker, and C. Wheldon, Phys. Rev. Lett. **113**, 012502 (2014).

[3] E. Epelbaum, H. Krebs, D. Lee, and Ulf-G. Meißner, Phys. Rev. Lett. **106**, 192501 (2011).

[4] Y. Kanada-En'yo, Progr. Theoret. Phys. **117**, 655 (2007).

[5] S. Ishikawa, Phys. Rev. C **90**, 061604(R) (2014).

[6] H. Morinaga, Phys. Lett. **21**, 78 (1966).

[7] M. Freer and H. O. U. Fynbo, Prog. Part. Nucl. Phys. **78**, 1 (2014).

[8] M. Freer, A. H. Wuosmaa, R. R. Betts, D. J. Henderson, P. Wilt, R. W. Zurmühle, D. P. Balamuth, S. Barrow, D. Benton, Q. Li, Z. Liu, and Y. Miao, Phys. Rev. C **49**, R1751 (1994).

[9] Ad. R. Raduta *et al.*, Phys. Lett. B **705**, 65 (2011).

[10] O. S. Kirsebom, M. Alcorta, M. J. G. Borge, M. Cubero, C. Aa. Diget, L. M. Fraile, B. R. Fulton, H. O. U. Fynbo, D. Galaviz, B. Jonson, M. Madurga, T. Nilsson, G. Nyman, K. Riisager, O. Tengblad, and M. Turrión, Phys. Rev. Lett. **108**, 202501 (2012).

[11] J. Manfredi, R. J. Charity, K. Mercurio, R. Shane, L. G. Sobotka, A. H. Wuosmaa, A. Banu, L. Trache, and R. E. Tribble, Phys. Rev. C **85**, 037603 (2012).

[12] T. K. Rana, S. Bhattacharya, C. Bhattacharya, S. Kundu, K. Banerjee, T. K. Ghosh, G. Mukherjee, R. Pandey, P. Roy, V. Srivastava, M. Gohil, J. K. Meena, H. Pai, A. K. Saha, J. K. Sahoo, and R. M. Saha, Phys. Rev. C **88**, 021601(R) (2013).

[13] M. Itoh, S. Ando, T. Aoki, H. Arikawa, S. Ezure, K. Harada, T. Hayamizu, T. Inoue, T. Ishikawa, K. Kato, H. Kawamura, Y. Sakemi, and A. Uchiyama, Phys. Rev. Lett. **113**, 102501 (2014).

[14] D. Dell'Aquila *et al.*, Phys. Rev. Lett. **119**, 132501 (2017).

[15] R. Smith, T. Kokalova, C. Wheldon, J. E. Bishop, M. Freer, N. Curtis, and D. J. Parker, Phys. Rev. Lett. **119**, 132502 (2017).

[16] O. Kirsebom, Physics **10**, 103 (2017).

[17] G. Giuliani, H. Zheng, and A. Bonasera, Prog. Part. Nucl. Phys. **76**, 116 (2014).

[18] A. Bonasera, F. Gulminelli, and J. Molitoris, Phys. Rep. **243**, 1 (1994).

[19] H. Suno, Y. Suzuki, and P. Descouvemont, Phys. Rev. C **94**, 054607 (2016).

[20] K. Schmidt *et al.*, Phys. Rev. C **95**, 054618 (2017).

[21] J. Mabiala, H. Zheng, A. Bonasera, Z. Kohley, and S. J. Yennello, Phys. Rev. C **94**, 064617 (2016).

[22] P. Marini *et al.* (INDRA Collaboration), Phys. Lett. B **756**, 194 (2016).

[23] Z. Kholey, Ph.D. thesis, Texas A&M University, 2010.

[24] V. Efimov, Phys. Lett. B **33**, 563 (1970).

[25] V. Efimov, Nat. Phys. **5**, 533 (2009).

[26] C. H. Greene, Phys. Today **63**, 40 (2010).

[27] M. Zaccanti, B. Deissler, C. D'Errico, M. Fattori, M. Jona-Lasinio, S. Müller, G. Roati, M. Inguscio, and G. Modugno, Nat. Phys. **5**, 586 (2009).

[28] https://cyclotron.tamu.edu/nimrod.

[29] S. Zhang, J. C. Wang, A. Bonasera, M. R. Huang, H. Zheng, G. Q. Zhang, Z. Kohley, Y. G. Ma, and S. J. Yennello, Chinese Phys. C **43**(6), 064102 (2019).

[30] P. Naidon and S. Endo, Rep. Prog. Phys. **80**, 056001 (2017).

[31] H. Zheng, A. Bonasera, M. Huang, and S. Zhang, Phys. Lett. B **779**, 460 (2018).

[32] http://www.nndc.bnl.gov.

[33] H. G. Schuster, *Deterministic Chaos* (Weinheim, New York, 1995).

[34] A. Tumino, A. Bonasera, G. Giuliani, M. Lattuada, M.Milin, R. G. Pizzone, C. Spitaleri, and S.Tudisco, Phys. Lett. B **750**, 59 (2015).

[35] H. Zheng and A. Bonasera, arXiv:1811.10412.